Taming of self-organization in highly confined soft matter to sub-100 nm scales: nanolens-arrays by spinodal instability of thin polymer films for high-resolution optical imaging

Ankur Verma[1,2] and Ashutosh Sharma[1,*]

[1]Department of Chemical Engineering, Indian Institute of Technology Kanpur, Kanpur 208 016, India
[2]Present address: Department of Chemical and Biomolecular Engineering, Johns Hopkins University, Baltimore, MD, 21211, USA

We present a mini review of the recent progress in the fabrication of nanolenses and their use for high-resolution optical imaging beyond the diffraction limit. Nanolenses break the diffraction limit by capturing near-field evanescent waves and refocusing them in the far-field image plane. The focus of this article is on our recent work on fabrication of nanolens and ordered lens arrays by a combination of the top-down and self-organization in unstable thin polymer films. Highly confined, thin (<50 nm) liquid polymer films spontaneously transform into microscale patterns of droplets by a spinodal instability leading to dewetting. The lateral length scales of these self-organized structures in air are limited by the weak van der Waals destabilizing force and a strong surface tension-induced stabilization. Limitations on slow dewetting kinetics and relatively large (>1 μm) length scales can be overcome by dewetting induced under an optimal mix of a non-solvent (water) and a good solvent, which reduces the interfacial tension without a concurrent solubilization of the polymer. This room temperature technique reduces both the time and the length scales of self-organized structures by over one order of magnitude. Further, directed dewetting combined with physico-chemically patterned substrates and films by e-beam, photolithography, laser ablation and nanoimprint lithography techniques can be used for fabrication of ordered nanostructures such as arrays of nanolenses.

Keywords: Dewetting, diffraction limit, high-resolution optical imaging, nanolens array.

LIGHT microscopy has been an integral tool for visualizing objects not visible to human eyes for almost four centuries. However, during the last five decades, the alternative microscopies such as electron microscope and scanning probe microscope have also become popular owing to the ever-increasing importance of smaller scales. In 1873, Ernst Abbe proposed the theory of image formation which showed that the resolution of an optical component is limited by the spreading of light through each point in the image plane, what is now known as the diffraction limit[1]. The resolution limit given by Abbe's equation is

$$d = \frac{0.612\lambda}{n \sin \alpha}, \tag{1}$$

where d is the resolution limit, λ wavelength of light, n the refractive index of the medium and α the half angle of the cone of light from the specimen plane accepted by the objective lens. The denominator of the above equation is also referred to as the numerical aperture (NA). Thus, in the best possible scenario, the resolution of light microscope is limited to about half the wavelength of light used to illuminate the sample, which is >200 nm for visible white light. However, some of the unique capabilities of the optical microscope such as cost, ease of use, ambient operation, non-invasive imaging and real-time continuous imaging have helped maintain it as an indispensable imaging tool. Thus, exploration of strategies to overcome the optical diffraction limit has become important. The primary reason for the diffraction limit lies in the loss of the so-called near-field evanescent waves which decay exponentially in space and cannot contribute to the image formation in the far-field optics. These waves carry sub-wavelength details of the object to be imaged and it is thus crucial to tap them for imaging beyond the diffraction limit[2]. In recent years, the diffraction limit has been overcome by methods such as single-molecule fluorescence[3], surface plasmon excitation through superlenses or hyperlenses[4–9] and near-field optical microscopy[10–17].

In terms of resolution, applicability and ease-of-use in bright field microscopy, near-field microscopes have

*For correspondence. (e-mail: ashutos@iitk.ac.in)

distinct advantages over other methods. Although the original idea of a near-field microscope was first proposed in 1928 by Synge[10,11], it was not until 1972 that the diffraction limit was first broken albeit for a significantly larger radio wave ($\lambda = 3$ cm)[12]. The first working near-field scanning optical microscope (NSOM) was developed in 1984, soon after the invention of the scanning probe microscope[13]. Over the years, NSOM has improved and integrated with better and faster electronics to resolve features smaller than 50 nm ($\sim\lambda/10$). However, a major limitation of any scanning probe method is the speed of measurements, which makes continuous real-time imaging over large areas difficult.

Recently, it has been demonstrated by several groups that a nanolens in conjunction with the normal bright field microscope can help break the diffraction limit by capturing the near-field evanescent waves which otherwise decay exponentially and would not have reached the image plane[14–17]. Therefore, one can do real-time continuous imaging with a regular microscope and yet achieve sub-diffraction limit resolution with the help of an array of nanolenses positioned in contact with the object. Figure 1 is a schematic diagram showing a nanolens working with a bright field microscope in the transmission mode. The nanolens helps in capturing the high-frequency evanescent waves, thus overcoming the diffraction limit.

Nanolens fabrication methods explored thus far can be divided in two categories: self-assembly (bottom-up)-based methods and lithography (top-down)-based methods. While the lithography-based methods provide precise positioning of nanolenses, they are limited by the choice of materials, configurability, dimensions (usually >1 μm), cost and difficulties in fabricating a smooth lens profile. Self-assembly-based methods give flexibility to the size and shape of nanolenses, but less precise positioning and size distribution remain as challenges. Next, we discuss some of these methods briefly to highlight their strengths and limitations.

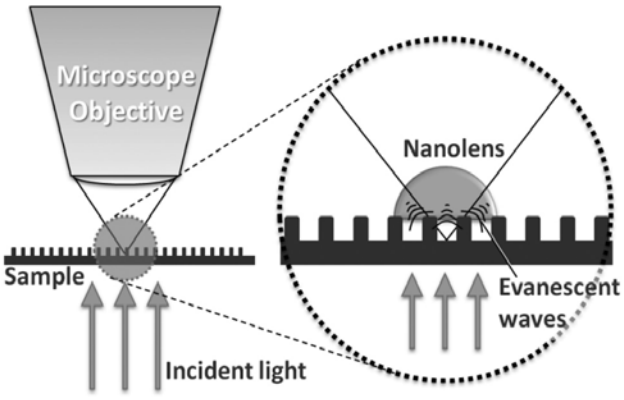

Figure 1. Schematic diagram of a nanolens working with optical microscope in transmission mode. Nanolens helps in improving optical resolution by capturing evanescent waves.

In a recent report, Lee *et al.*[14] have demonstrated the near-field high resolution achieved by spherical nanolenses that are made by the self-assembly of organic molecules. These nanolenses exhibit curvilinear trajectories of light which leads to extremely short focal lengths, allowing resolution of features beyond the diffraction limit by the near-field magnification. For the lens assembly, these authors[14] used calix hydroquinone (CHQ) which is composed of four *p*-hydroquinone subunits and eight hydroxyl groups. Intermolecular hydrogen bonds and π–π stacking interactions are the critical intermolecular forces responsible for the self-assembly of CHQ molecules into supramolecular nanolenses. To make these nanolenses, CHQ monomer is dissolved in 1 : 1 water–acetone solution and slowly heated from –14°C to 40°C in aqueous environment for a day. This process forms self-assembled spherical nanostructures with diameter ranging from 50 nm to 3 μm. The plano-convex nanolenses thus formed can be isolated and then placed on the optical device with the help of a dual focused ion beam. The CHQ nanolenses break the diffraction limit to resolve lines separated by ~200 nm using conventional optical microscope. The study also investigated the relative magnification/resolution in the face-up and face-down configurations of the plano-convex nanolenses on the imaging object. While the process is rather complex and time-intensive, it was among the first attempts to use nanolenses in conjunction with optical microscopy.

Later, Wang *et al.*[16] reported resolutions of less than 100 nm in bright field microscope with the help of micrometre-sized glass beads. They used ordinary glass (refractive index $n = 1.46$) microspheres of diameter between 2 and 9 μm. These far-field super-lenses achieved resolutions between $\lambda/8$ and $\lambda/14$, and magnification between ×4 and ×8. The study could successfully resolve 100 nm tracks on a blu-ray disc and 90 nm corners of a star-shaped object. These microsphere super-lenses can be integrated with a normal optical microscope in both transmission and reflection modes and work under white light illumination. The study also claimed that it is in principle possible to image features as small as 20 nm with the help of a 5 μm super-lens made of a material with the refractive index of 1.8. This would indeed be a remarkable advance as it will open up a variety of applications such as imaging of viruses, interior of living cells and DNA by conventional microscopes without the need of fluorescence tagging. Assembling of the micrometre-sized glass beads in the form of an array, so that the imaging can be performed over larger area, still needs to be addressed. Further, the large size of the beads limits the field of view significantly.

Recently, Kang *et al.*[17] have demonstrated a method to produce an array of microlenses with diameter ranging from ~500 nm to ~15 μm and a wide range of curvatures (contact angle: 10°–90°) using a photocurable polymer. They fabricated the microlens array by direct transfer

of partially cured polymer to the surface and were able to resolve nanoscale gaps of 130 nm. The fabrication method involves three successive steps: first, a flexible polydimethylsiloxane (PDMS) stamp with protruding pillars is soaked with a photocurable transparent polymer. Then this stamp is used to deposit polymer droplets on the pre-treated target surface by applying a nominal pressure (~10 Pa). These droplets were then allowed to reach the equilibrium contact angle, which depends on the substrate wettability. Finally, the structures were made permanent by crosslinking of polymer by UV exposure. Size of the droplets was controlled by changing the feature size on the stamp and by regulating the amount of polymer on the stamp, whereas the shape of these droplets was controlled by surface treatment. To attain high contact angles, the target surface was coated with Teflon thin-film (~5 nm). The photosensitive polymers used were polyurethane acrylate (PUA), Norland Optical Adhesive (NOA) and polyethylene glycol diacrylate (PEG). The minimum contact angle (9.8°) droplets were of PUA on glass, whereas the maximum contact angle (90.9°) was achieved with PEG on Teflon. The method can be applied to assemble a microlens array directly on a variety of complex surfaces to be imaged such as lenticular, stepped and cicada wings. These lenses were used to resolve honeycomb-like structures with 500 nm periodicity and a smallest gap of 130 nm using 150× objective lens with NA of 0.9. The report also studied systematically the magnifying effect of these lenses. Although this method demonstrates the fabrication of different sized lenses on a variety of surface geometries, the lens curvature is not tunable, but is governed by the wettability of the substrate. To achieve a particular shape of the lens, appropriate combinations of surface and the lens material have to be used, which limits the applicability of the process in many situations.

There are other reported methods of making microlenses, such as thermal reshaping of colloidal particles[18], solvent exchange precipitated particles[19], inkjet printing of liquid droplets and subsequent polymerization[20], stimuli responsive hydrogels[21] and liquid-filled microchannels[22], all of which have been proposed in the last few years as potential candidates for scalable production of microlens arrays.

In contrast to the top-down fabrication methods described above, we have recently demonstrated a simple and versatile method for making nanolenses and arrays by controlling the instability and self-organized dewetting of ultrathin (<50 nm) polymer films[15]. Self-organization may be defined as the predilection of an unstable system to spontaneously morph into a (usually) more complex shape by a re-organization of its material by flow and deformation fueled by energy minimization. Highly confined nanosystems, such as an ultrathin (<100 nm) film, are often unstable owing to their high pent-up surface energy and attractive/repulsive intersurface interactions because of the close proximity of interfaces within the decay lengths of interactions such as the van der Waals, electrostatic, etc. Thus, in addition to the two established paradigms of nano-fabrication – top-down and bottom-up (self-assembly) – the third alternative of self-organization is becoming increasingly attractive for nanofabrication in soft materials. In particular, much attention has been devoted to the instability and spontaneous pattern formation in thin films of soft materials such as polymer and metal melts and solutions and soft elastomers and gels. Clearly, the material should be sufficiently soft in order for the self-organization in a thermodynamically unstable system to proceed by flow and deformation on relatively fast, practical timescales. Thus, self-organization in thin polymer films, produced for example by spin coating, can occur if the as-deposited solid film is first softened by thermal annealing beyond its glass transition or by contacting with a solvent vapour to reduce its glass transition temperature below room temperature. Once the polymer chains acquire sufficient mobility, an unstable thin film can dewet its substrate to form a pattern. Dewetting of a thin film involves surface instability and spontaneous break-up of an unstable thin (<100 nm) liquid film to produce an array of holes that grow and coalesce to eventually form droplets. This process has been studied extensively over the last three decades[23–38]. The shape of these liquid droplets is similar to a plano-convex lens and 'freezing' of the droplet shapes by cooling, cross-linking, etc. allows their use as nanolenses for imaging. A polymer (e.g. polystyrene, polymethylmethacrylate (PMMA)) thin film ($h < 100$ nm) on a non-wetting substrate undergoes spontaneous dewetting when heated above its glass transition temperature (T_g) or exposed to the solvent vapour, which increases the polymer mobility for reorganization. These polymers are in glassy state at room temperature or when not in contact with a solvent vapour so that a 'liquid' shape can be frozen to remain in a particular shape suitable for imaging. However, there have been several serious limitations on dewetting of polymer thin films in air: (1) droplets produced have very low equilibrium contact angle (<30°) and thus large radii of curvature; (2) the length scale of instability and thus the size/spacing of the resulting droplets are rather large (>10 μm), which limits their use as nanolens, (3) the dewetting kinetics is slow and takes several hours for dewetting to complete and (4) heating of the film and cooling of droplets may result in residual stresses and distortions. The limitations on the large length scale and slow kinetics of instability are imposed by the dominant stabilizing influence of surface tension in thin films and a weak destabilization engendered by the long-range intersurface van der Waals attraction. In recent studies, we demonstrated a novel room temperature technique to overcome all of these challenges on the length and timescales of self-organization by carrying out dewetting under an optimal mix of a nonsolvent (water) and organic

solvents[15,39–41]. As discussed below, the technique also allows control on the size and shape of the resulting droplets. In order to fully appreciate the technique, we first present a brief introduction to the self-organized dewetting of a thin liquid film.

Self-organized dewetting of polymer thin films is engendered by attractive inter-surface forces such as van der Waals and opposed by the surface tension. A competition between the destabilizing and stabilizing factors determines the wavelength (length scale) of the surface instability that is given by[27]

$$\lambda_{\mathrm{L}} = \left[\frac{8\pi^2 \gamma}{-(\partial\varphi / \partial h)} \right]^{1/2}, \qquad (2)$$

where γ is interfacial tension, φ the inter-surface destabilizing potential ($\varphi \sim h^{-3}$ for the van der Waals attraction) and h is the film thickness[27]. As the instability grows, it leads to the formation of isolated holes in the film. These holes grow in size as time progresses and eventually coalesce to form a connected network of polymer ribbons, which finally breaks into the isolated droplets of polymer. Interfacial tension γ, opposes the creation of new surface formed by the growth of instability in the form of increasing surface deformations. Physically, λ_{L} depicts the average distance between two holes, which is roughly also the average distance between two droplets at a later stage of instability. In order to reduce λ_{L} (as well as the droplet size), interfacial tension should be very small and the destabilizing potential should be high. Solving eq. (2) for a potential φ gives $\lambda_{\mathrm{L}} \sim h^n$ type dependence of wavelength on film thickness. For example, in the case of the apolar van der Waals interaction, $\varphi \sim h^{-3}$ and thus n equals 2 from eq. (2). However, more complex scenarios are encountered when the polar interactions are involved as in immersion of the film in a liquid polar solvent[38]. The dependence of λ_{L} on the film thickness, h as given in eq. (2) implies that the distance between droplets and the droplet size can be controlled by just changing the initial film thickness[27].

As discussed above, reduction of the feature size in self-organized dewetting requires that the inter-facial tension should be very low and the destabilizing inter-surface potential should be high. A straightforward way to reduce the surface tension to nearly zero is to immerse the polymer film in a good solvent. However, it would also mean dissolution of the polymer film rather quickly, so that there is nothing left to organize! These conflicting demands can be balanced by a simple approach in which the film is immersed in a mixture of a good solvent and a non-solvent whose composition is tuned in such a way that the polymer is only sparingly soluble in the mixture, but the good solvent can now diffuse in the polymer and reduce both its glass transition temperature and its inter-facial tension. In recent works[15,39–41], we proposed such a intensified self-organized dewetting in which a thin polymer film of polystyrene or PMMA is immersed in a mixture of water (non-solvent), methyl ethyl ketone (MEK; good solvent) and acetone (poor solvent) in the ratio 15 : 7 : 3 respectively. Acetone was added to make a homogeneous mixture of methyl ethyl ketone and water. The solvent molecules diffuse in the polymer matrix and make it liquid-like at room temperature. However, water being the major constituent of the liquid phase, dissolution of the polymer is prevented. A major influence of this water–organic solvent mixture is to reduce the inter-facial tension by nearly two orders of magnitude[15,39–41]. In addition, the strength of the destabilizing force field is enhanced by inducing a longer-range electrostatic ($\varphi \sim h^{-2}$) attraction acquired because of the charging of the film surface in the liquid mix[39]. This leads to more than an order of magnitude decrease in λ_{L} and the droplet diameter; tremendous increase in the contact angle and significantly faster dewetting dynamics[15,39]. As the dewetting progresses, the contact angle changes from a very low value (~30°) to its equilibrium value in water–solvent mix (~150°) in about 1 h and the droplet shape at any intermediate step can be frozen by just removing it from the liquid and drying. This change in droplet shape is fully reversible, and thus, a droplet of lower contact angle (higher radius of curvature) is readily recovered by heating in air above the T_{g} (~110°C) or by exposure to a solvent vapour. The rate of change of the contact angle is controlled by viscosity of the polymer, which is a function of its molecular weight[39].

The droplets of size in the range 300 nm–3 μm could be produced by dewetting of 15–60 nm thick polystyrene thin films[15,39–41]. Figure 2 shows transverse field emission scanning electron microscope (FESEM) images of some of the droplets with base-radii from 370 nm to 2.9 μm and contact angle from 30° to 143° (ref. 15). This demonstrates the continuous ranges of the size and shape that can be engineered without changing the substrate or the lens material. The only control variables here are the initial film thickness and the time after which a lens is frozen.

We have also demonstrated that these droplets after being removed from dewetting solution and annealed to achieve a smooth spherical shape can be used as nanolenses to produce ultrahigh magnification under conventional light microscope[15]. Figure 3 shows that it is possible to resolve stripes on the substrate that are otherwise not visible. One of the notable advantages of this method is that it can be used by just placing a thin, optically transparent substrate with nanolenses over the imaging object. This add-on microscope aide is reusable and in other cases, it can also be assembled *in situ* to form directly on the surface to be imaged. There is also no need to use sophisticated tools for placing individual lenses on the substrate as required in some of the other methods described earlier.

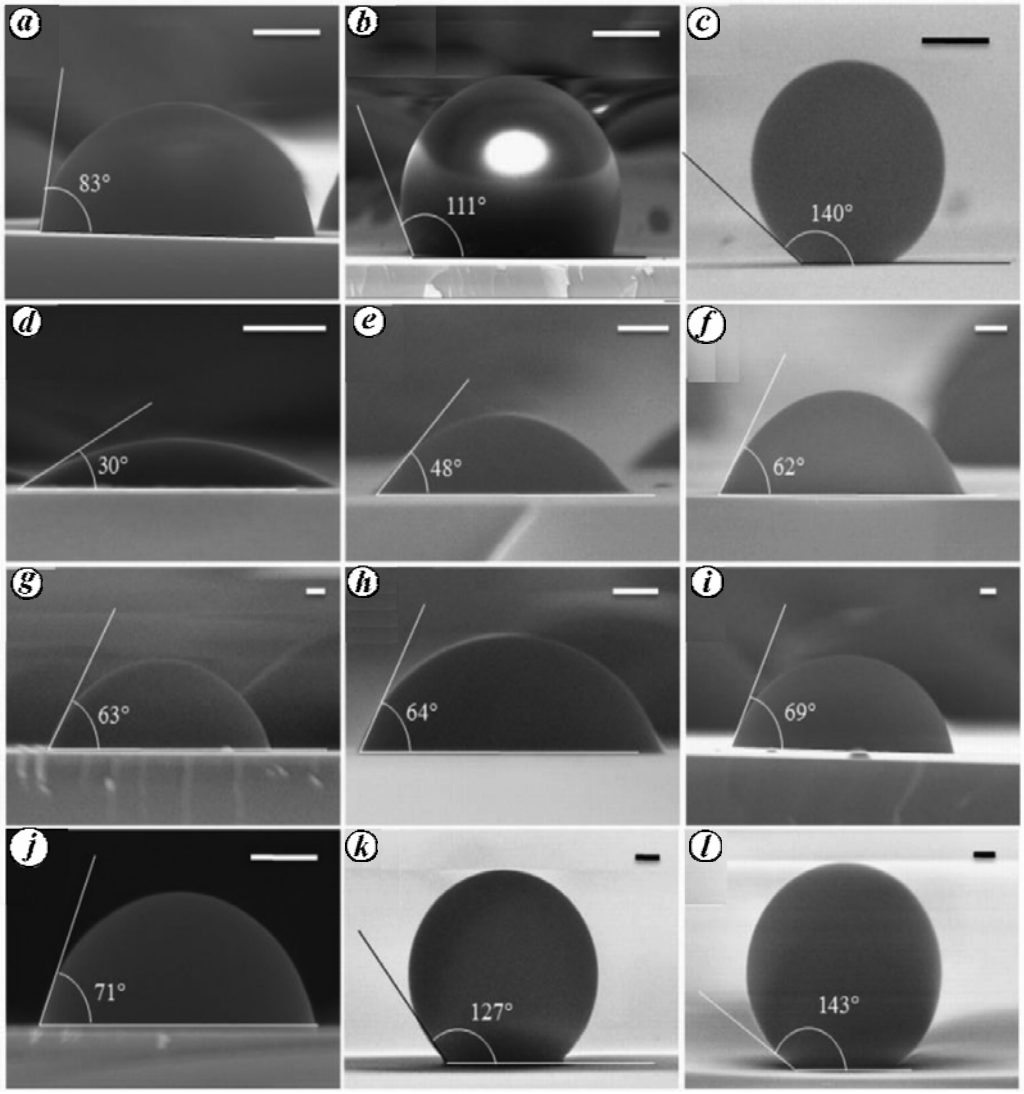

Figure 2. Transverse FESEM images of PS droplets. ***a*–*c***, Temporal evolution of a droplet obtained by dewetting of a 25 nm thick PS film on a flat silicon substrate. Contact angle after: (***a***) 15 min is 83°, (***b***) 20 min is 111° and (***c***) 1 h is 140°. ***d*–*l***, A range of droplet shapes and sizes obtained by dewetting of 14–60 nm thick films. Their base-radii range from 370 nm to 2.9 μm and the contact angle varies from 30° to 143° (scale bar: 200 nm). Reproduced from Verma and Sharma[15].

As these nanolenses are already shown to overcome the diffraction limit, the next step is to build ordered arrays of nanolenses so that the imaging over a large area can be done. To this end, we have worked on creating uniformly spaced nanolens arrays by integrating self-organized dewetting with the widely used top-down fabrication methods as discussed below[15,39–41]. Dewetting of a homogeneously flat thin film on a smooth defect-free surface produces polydispersed droplets that are randomly distributed on the surface, but with a mean inter-droplet spacing close to or correlated to λ_L. A spatially ordered array of droplets can be fabricated by localizing the initial instability (formation of holes) by a micro/nano patterned template, where the template pattern periodicity is close to the wavelength of the instability (λ_L). Dewetting on a physico-chemically patterned surface has been studied both theoretically and experimentally in the last decade[42–51]. The physico-chemical heterogeneity acts as the nucleation site for the initial hole formation as the instability grows in the film. This leads to the formation of ordered array of droplets as long as the periodicity of the physico-chemical pattern is comparable to λ_L for that particular film on a flat surface[39–41]. Figure 4 shows one such ordered array of nanolenses of size 200 nm with 1 μm periodicity that was achieved by dewetting of a 25 nm thick polystyrene film on a physically patterned substrate. In Figure 4 *a*, the bright smaller spots are the pillars fabricated using electron beam lithography (EBL) on which a polymer thin film was coated and subsequently dewetted. Bigger and darker spots are nanolenses which are near-perfectly arranged in an array. Dewetting is initiated on top of the pillars where the film thickness is minimum.

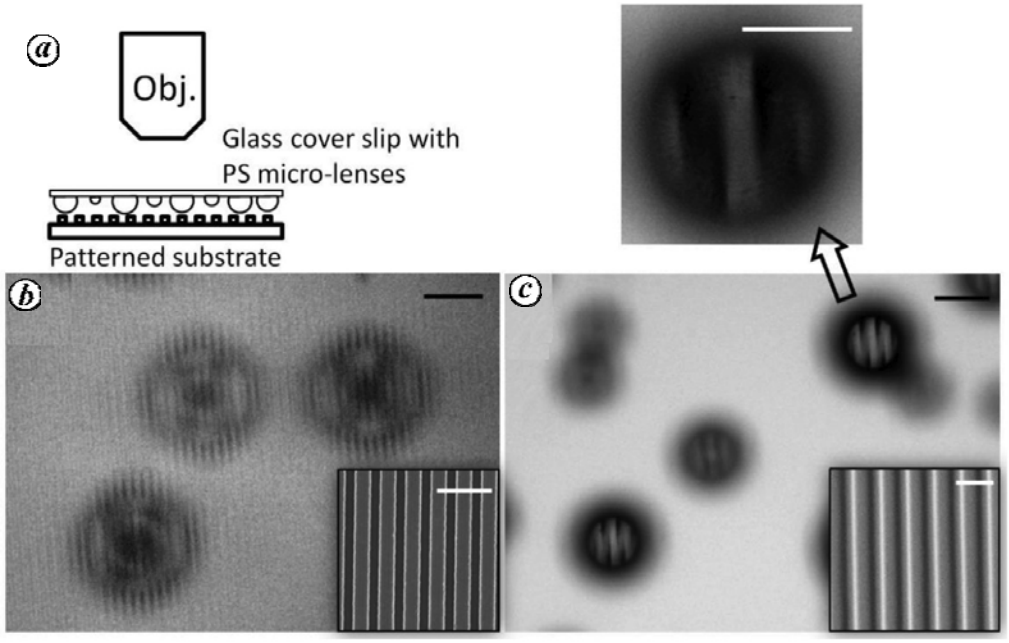

Figure 3. Resolution of striped patterns in optical microscope by PS micro-lenses. ***a***, Schematic diagram of imaging using optical microscope. ***b***, 500 nm wide strips on silicon wafer resolved by 50X objective (NA/0.5). (Inset) FESEM image of the object. ***c***, CD strips with channel width of 800 nm resolved by 20X (NA/0.4) objective, enlarged view is of 50X objective. (Inset) FESEM image of the object. Scale bar: 5 μm (black), 2 μm (white). Reproduced from Verma and Sharma[15].

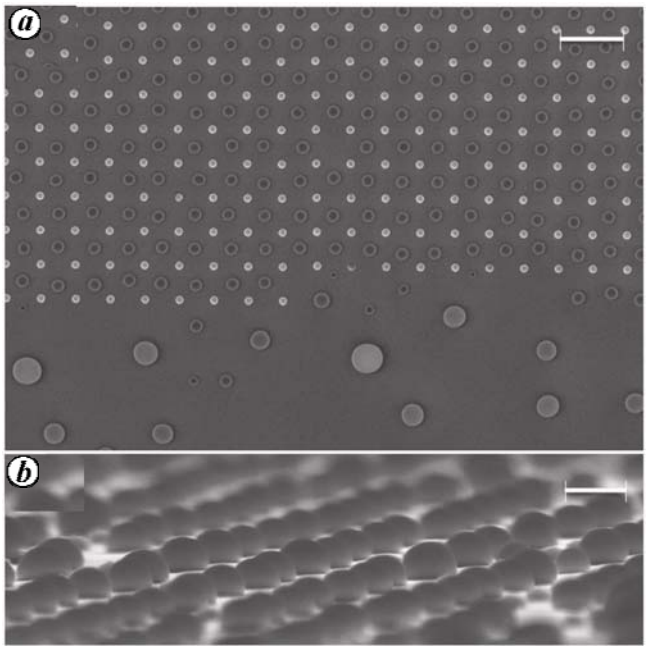

Figure 4. Dewetting on a physically patterned substrate. ***a***, FESEM image of the dewetted structure (scale bar: 2 μm). ***b***, Transverse view showing arrays of dewetted droplets (scale bar: 500 nm). Reproduced from Verma and Sharma[15].

Figure 4 *b* shows the transverse view of the same nanolens array[15].

Although a physico-chemically patterned substrate template can be used to produce nanolens arrays over a large area, this method is not particularly suitable in that a new template first needs to be fabricated for each lens array. In addition, micro/nano patterning of substrates other than silicon wafers can be a more involved multistep process. The ideal process for nanolens array fabrication should be fast, portable across a variety of materials and involve minimum steps and complexity. A method which comes closer to the ideal in producing the nanolens arrays on the flat homogeneous surfaces employs creation of differential wetting contrast by exposing the film to extremely low doses of electron beam (e-beam)[40,41].

The method works by creation of a differential viscosity contrast in the nanodomains of the polymer film created by selected-area e-beam exposure. A negative contrast polymer such as polystyrene exhibits higher viscosity in the e-beam exposed region, so the dewetting dynamics becomes slower in the exposed part. Therefore, dewetting starts in unexposed regions of the films and if the periodicity of e-beam pattern matches with λ_L of the film, we get nanolenses corresponding to the exposed regions. In a positive contrast polymer such as PMMA, this phenomenon is reversed and the e-beam exposed regions of the film dewet faster. Figure 5 shows nanolens arrays obtained by dewetting of 6.5 and 12 nm thick PS films which were exposed with e-beam in a dot pattern. The e-beam doses required for this method are at least ten times smaller compared to those required for EBL. This makes the process significantly faster and realistic for large-area nanolens arrays. Just to give a perspective on

how fast this method is, a single e-beam can fabricate around half a million nanolenses per second. The minimum dimensions of the polymeric domains created by this method were ~40 nm (ref. 41), thus breaking the sub-100 nm limit for the first time in the self-organized dewetting of a polymer layer.

The self-organized dewetting to produce nanodomains requires only that the thin film deposited is unstable owing to attractive inter-surface interactions such as the van der Waals, electrostatic or others between its two interfaces. The method is thus portable across a variety of materials in that it does not depend on the precise chemical nature of the material. For example, similar nanolens arrays could also be fabricated by dewetting of e-beam modified thin films of other polymers such as PMMA. PMMA is a positive tone e-beam resist, meaning that its viscosity decreases in the e-beam exposed regions. Thus, the thin film instability grows faster in the e-beam exposed domains of PMMA. As MEK is also a good solvent for PMMA, the same dewetting mixture (water, MEK and acetone in the ratio 15 : 7 : 3) also produces selective dewetting of the e-beam exposed regions. Figure 6 *a* shows an array of 204 ± 14 nm sized nanolenses with 750 nm periodicity obtained by dewetting of a 15 nm thick PMMA film. Figure 6 *b* shows an array of 2.9 ± 0.2 μm sized nanolenses with 15 μm periodicity obtained by dewetting of a 27 nm thick PMMA film. In both the cases, the nanolenses produced are highly monodispersed and defects in the 2D arrays are rather rare.

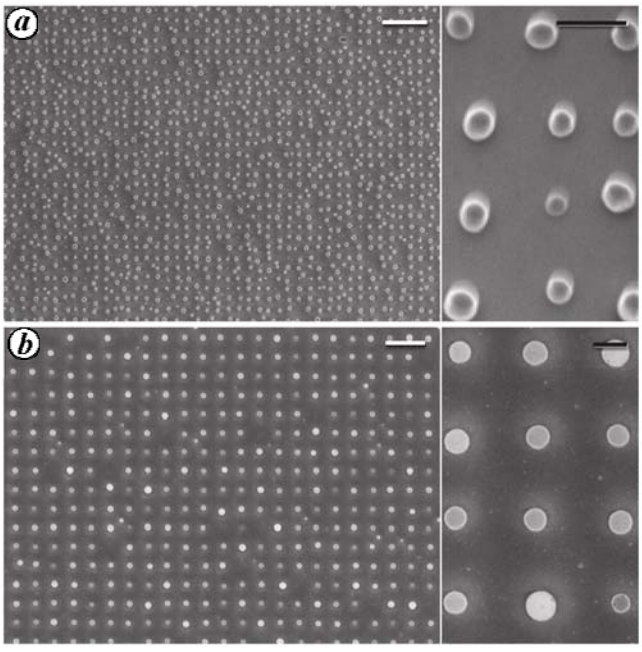

Figure 5. Two-dimensionally aligned droplets obtained after dewetting of e-beam modified PS thin film: (***a***) 6.5 nm thick PS film and (***b***) 12 nm thick PS film (scale bar: white is 1 mm and black is 200 nm). Reproduced by permission of The Royal Society of Chemistry from Verma and Sharma[40].

In conclusion, we have summarized some recent techniques of fabrication of nanolens arrays using top-down and bottom-up nanofabrication, with a focus on a third technique of self-organized, directed dewetting of ultrathin polymer films. Self-organization in a thermally annealed ultrathin (<50 nm) liquid polymer film in air produces shallow lenses of tens of micrometre dimension with a slow kinetics. We show that spontaneous dewetting of an ultrathin (<50 nm) polymer film under a mixture of a good solvent and a non-solvent overcomes the limitations on the length and timescales for spontaneous dewetting. Pushing down the limits of self-organization to below 100 nm is made possible by orders of magnitude reduction in the stabilizing influence of interfacial tension and by strengthening of the destabilizing force. Further, it is a room temperature technique that obviates the need for heating of the film and cooling of the droplets, which may result in residual stresses and distortions. Self-organized dewetting thus appears to be among one of the most versatile methods in terms of controlling the size and shape of the nanolenses continuously from less than 50 nm to several micrometres and the base-angles

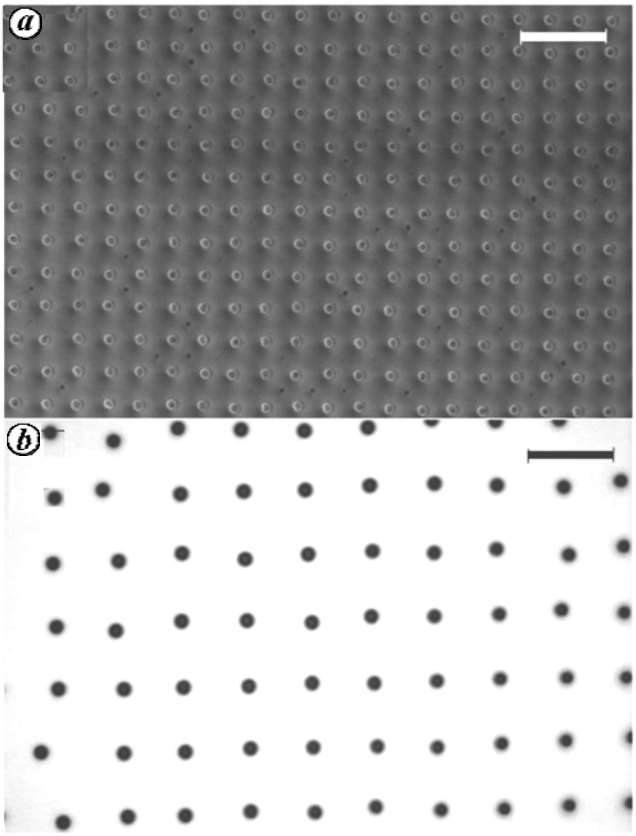

Figure 6. PMMA nanolens arrays fabricated by e-beam assisted dewetting of thin PMMA films. ***a***, SEM image of 204 nm (±14 nm) nanolens array obtained by dewetting of a 15 nm thick PMMA film. (scale bar: 2 μm). ***b***, Optical micrograph of 2.9 μm (±0.2 μm) nanolens array obtained by dewetting of 27 nm thick PMMA film (scale bar: 20 μm).

ranging from 30° to 150°. While it provides a significantly cost-effective and scalable method to form nanolens arrays, there are some issues yet to be addressed. Generally, the nanolens arrays for imaging should be most effective in covering the maximal area when the lenses are in close-pack configuration. One possible approach to achieve that using self-organized dewetting is the multistep deposition of nanolens array of compatible polymers by filling out the vacant area in each step. Using EBL, one such possibility is the dewetting of a multilayered polymer thin film, where each layer of polymer has different electron beam contrast. The arrays of nanolenses of tunable size and curvature (~40 nm–10 μm) fabricated by directed and enhanced dewetting of ultrathin (5–50 nm) polymer films may also find applications ranging from the near-field imaging, 'compound eye', amplification of weak optical signals, sub-wavelength lithography to fundamental studies of nanooptics. Further, the technique also offers the possibility of precise positioning of functional materials or their precursors in ordered nanodomains using the polymer as a delivery vehicle.

1. Murphy, D. B. and Davidson, M. W., Diffraction and spatial resolution. In *Fundamentals of Light Microscopy and Electronic Imaging*, Wiley-Blackwell, Hoboken, USA, 2012, 2nd edn, pp. 103–111.
2. Zheludev, N. I., What diffraction limit? *Nature Mater.*, 2007, **7**, 420–422.
3. Hell, S. W., Far-field optical nanoscopy. *Science*, 2007, **316**, 1153–1158.
4. Zhang, X. and Liu, Z., Superlenses to overcome the diffraction limit. *Nature Mater.*, 2007, **7**, 435–441.
5. Smolyaninov, I. I., Hung, Y.-J. and Davis, C. C., Magnifying superlens in the visible frequency range. *Science*, 2007, **315**, 1699–1701.
6. Liu, Z., Lee, H., Xiong, Y., Sun, C. and Zhang, X., Far-field optical hyperlens magnifying sub-diffraction-limited objects. *Science*, 2007, **315**, 1686.
7. Fang, N., Lee, H., Sun, C. and Zhang, X., Sub-diffraction-limited optical imaging with a silver superlens. *Science*, 2005, **308**, 534–537.
8. Pendry, J. B., Negative refraction makes a perfect lens. *Phys. Rev. Lett.*, 2000, **85**, 3966–3969.
9. Tripathi, A., Chokshi, T. V. and Chronis, N., A high numerical aperture, polymer-based, planar microlens array. *Opt. Express*, 2009, **17**, 19908.
10. Synge, E. H., A suggested method for extending the microscopic resolution into the ultramicroscopic region. *Philos. Mag.*, 1928, **6**, 356.
11. Synge, E. H., An application of piezoelectricity to microscopy. *Philos. Mag.*, 1932, **13**, 297.
12. Ash, E. A. and Nicholls, G., Super-resolution aperture scanning microscope. *Nature*, 1972, **237**, 510.
13. Pohl, D. W., Denk, W. and Lanz, M., Optical stethoscopy: image recording with resolution $\lambda/20$. *Appl. Phys. Lett.*, 1984, **44**, 651.
14. Lee, J. Y. *et al.*, Near-field focusing and magnification through self-assembled nanoscale spherical lenses. *Nature*, 2009, **460**, 498–501.
15. Verma, A. and Sharma, A., Enhanced self-organized dewetting of ultrathin polymer films under water–organic solutions: fabrication of sub-micron spherical lens arrays. *Adv. Mater.*, 2010, **22**, 5306–5309.
16. Wang, Z. *et al.*, Optical virtual imaging at 50 nm lateral resolution with a white-light nanoscope. *Nature Commun.*, 2011, **2**, 218 (1–6).
17. Kang, D., Pang, C., Kim, S. M., Cho, H. S., Um, H. S., Choi, Y. W. and Suh, K. Y., Shape-controllable microlens array via direct transfer of photocurable polymer droplets. *Adv. Mater.*, 2012, **24**, 1709–1715.
18. Vlad, A., Huynen, I. and Melinte, S., Wavelength-scale lens microscopy via thermal reshaping of colloidal particles. *Nanotechnology*, 2012, **23**, 285708 (1–9).
19. Zhang, X., Ren, J., Yang, H., He, Y., Tan, J. and Qiao, G. G., From transient nanodroplets to permanent nanolenses. *Soft Matter*, 2012, **8**, 4314–4317.
20. Tien, C.-H., Hung, C.-H. and Yu, T.-H., Microlens arrays by direct-writing inkjet print for LCD backlighting applications. *J. Display Technol.*, 2009, **5**, 147–151.
21. Dong, L., Agarwal, A. K., Beebe, D. J. and Jiang, H. R., Adaptive liquid microlenses activated by stimuli-responsive hydrogels. *Nature*, 2006, **442**, 551–554.
22. Chronis, N., Liu, G. L., Jeong, K. H. and Lee, L. P., Tunable liquid-filled microlens array integrated with microfluidic network. *Opt. Express*, 2003, **11**, 2370–2378.
23. Reiter, G., Dewetting of thin polymer films. *Phys. Rev. Lett.*, 1992, **68**, 75–78.
24. Reiter, G., Unstable thin polymer films: rupture and dewetting processes. *Langmuir*, 1993, **9**, 1344–1351.
25. Sharma, A., Relationship of thin film stability and morphology to macroscopic parameters of wetting in the apolar and polar systems. *Langmuir*, 1993, **9**, 861–869.
26. Sharma, A., Equilibrium contact angles and film thicknesses in the apolar and polar systems: role of intermolecular interactions in coexistence of drops with thin films. *Langmuir*, 1993, **9**, 3580–3586.
27. Sharma, A. and Reiter, G., Instability of thin polymer films on coated substrates: rupture, dewetting and drop formation. *J. Colloid Interface Sci.*, 1996, **178**, 383–399.
28. Sharma, A. and Khanna, R., Pattern formation in unstable thin liquid films. *Phys. Rev. Lett.*, 1998, **81**, 3463–3466.
29. Sharma, A., Many paths to dewetting of thin films: anatomy and physiology of surface instability. *Eur. Phys. J. E*, 2003, **12**, 397–408.
30. Xie, R., Karim, A., Douglas, J. F., Han, C. C. and Weiss, R. A., Spinodal dewetting of thin polymer films. *Phys. Rev. Lett.*, 1998, **81**, 1251–1254.
31. Reiter, G., Khanna, R. and Sharma, A., Enhanced instability in thin liquid films by improved compatibility. *Phys. Rev. Lett.*, 2000, **85**, 1432–1435.
32. Herminghaus, S., Dynamical instability of thin liquid films between conducting media. *Phys. Rev. Lett.*, 1999, **83**, 2359–2361.
33. Seeman, R., Herminghaus, S. and Jacobs, K., Dewetting patterns and molecular forces. *Phys. Rev. Lett.*, 2001, **86**, 5534–5537.
34. Becker, J., Grun, G., Seemann, R., Mantz, H., Jacobs, K., Mecke, K. R. and Blossey, R., Complex dewetting scenarios captured by thin-film models. *Nature Mater.*, 2002, **2**, 59–63.
35. Seemann, R. *et al.*, Dynamics and structure formation in thin polymer melt films. *J. Phys.: Condens. Matter*, 2005, **17**, S267–S290.
36. Craster, R. V. and Matar, O. K., Dynamics and stability of thin liquid films. *Rev. Mod. Phys.*, 2009, **81**, 1131–1198.
37. Xu, L., Sharma, A. and Joo, S. W., Instability and pattern formation induced in thin crystalline layers of a conducting polymer P3HT by unstable carrier films of an insulating polymer. *J. Phys. Chem. C*, 2012, **116**, 21615–21621.
38. Xu, L., Sharma, A. and Joo, S. W., Dewetting of stable thin polymer films induced by a poor solvent: role of polar interactions. *Macromolecules*, 2012, **45**, 6628–6633.

39. Verma, A. and Sharma, A., Submicrometer pattern fabrication by intensification of instability in ultrathin polymer films under a water–solvent mix. *Macromolecules*, 2011, **44**, 4928–4935.
40. Verma, A. and Sharma, A., Self-organized nano-lens arrays by intensified dewetting of electron beam modified polymer thin-films. *Soft Matter*, 2011, **7**, 11119–11124.
41. Verma, A. and Sharma, A., Sub-40 nm polymer dot arrays by self-organized dewetting of e-beam treated ultrathin polymer films. *RSC Adv.*, 2012, **2**, 2247–2249.
42. Higgins, A. M. and Jones, R. A. L., Anisotropic spinodal dewetting as a route to self-assembly of patterned surfaces. *Nature*, 2000, **404**, 476–478.
43. Konnur, R., Kargupta, K. and Sharma, A., Instability and morphology of thin liquid films on chemically heterogeneous substrates. *Phys. Rev. Lett.*, 2000, **84**, 931–934.
44. Kargupta, K. and Sharma, A., Templating of thin films induced by dewetting on patterned surfaces. *Phys. Rev. Lett.*, 2001, **86**, 4536–4539.
45. Sehgal, A., Ferreiro, V, Douglas, J. F., Amis, E. J. and Karim, A., Pattern-directed dewetting of ultrathin polymer films. *Langmuir*, 2002, **18**, 7041–7048.
46. Kargupta, K. and Sharma, A., Mesopatterning of thin liquid films by templating on chemically patterned complex substrates. *Langmuir*, 2003, **19**, 5153–5163.
47. Geoghegan, M., Wang, C., Rhese, N., Magerle, R. and Krausch, G., Thin polymer films on chemically patterned, corrugated substrates. *J. Phys.: Condens. Matter*, 2005, **17**, S389.
48. Julthongpiput, D., Zhang, W., Douglas, J. F., Karim, A. and Fasolka, M. J., Pattern-directed to isotropic dewetting transition in polymer films on micropatterned surfaces with differential surface energy contrast. *Soft Matter*, 2007, **3**, 613–618.
49. Yoon, B., Acharya, H., Lee, G., Kim, H.-C., Huh, J. and Park, C., Nanopatterning of thin polymer films by controlled dewetting on a topographic pre-pattern. *Soft Matter*, 2008, **4**, 1467.
50. Mukherjee, R., Bandopadhyay, D. and Sharma, A., Control of morphology in pattern directed dewetting of thin polymer films. *Soft Matter*, 2008, **4**, 2086–2097.
51. Sehgal, A., Bandyopadhyay, D., Kargupta, K., Sharma, A. and Karim, A., From finite-amplitude equilibrium structures to dewetting in thin polymer films on chemically patterned substrates. *Soft Matter*, 2012, **8**, 10394–10402.

ACKNOWLEDGEMENTS. A.S. thanks the Department of Science and Technology, New Delhi for providing a grant to Thematic Unit on Soft Nanotechnology at IIT Kanpur and DRDO, New Delhi for funds. We thank John Wiley and Sons, and Royal Society of Chemistry for allowing reproduction of our previously published figures.

Received 19 July 2012; accepted 13 February 2013